Supporting Information

Plasmonic Coupling of Au Nanoclusters on a Flexible MXene/Graphene Oxide Fiber for Ultra-sensitive SERS Sensing

Xin Liu[1,2], Alei Dang[1,2*], Tiehu Li[1,2*], Yiting Sun [1,2], Tung-Chun Lee[3,4], Weibin Deng[1,2], Shaoheng Wu[1,2], Amir Zada[5], Tingkai Zhao[1,2], Hao Li[1,2]

[1.] School of Materials Science and Engineering, Northwestern Polytechnical University, Xi'an 710072, P. R China

[2.] Shannxi Engineering laboratory for Graphene New Carbon Materials and Applications, School of Materials Science and Engineering, Northwestern Polytechnical University, Xi'an 710072, P. R China.

[3.] Department of Chemistry, University College London (UCL), London WC1H 0AJ, U.K

[4.] Institute for Materials Discovery, University College London (UCL), London WC1H 0AJ, U.K

[5.] Department of Chemistry, Abdul Wali Khan University Mardan, 23200, Pakistan.

*Corresponding author：Alei Dang, Tiehu Li,

E-mail address: dangalei@nwpu.edu.cn; litiehu@nwpu.edu.cn

1. Synthesis of graphene oxide (GO)

The previously reported improved Hummers method was employed for the synthesis of GO. To improve the productivity of GO, a pre-oxidation process was used. Typically, 2 g graphite powder was slowly added to a solution containing 2 g potassium persulfide in H_3PO_4 (2 mL) and H_2SO_4 (22 mL) under continuous stirring and heated at 80 °C for 5 h. The solution was filtered, and the residues were washed with a large amount of DI water until the filtrate became neutral. The obtained pre-oxidized graphite was dried in an oven for further use. The dried pre-oxidized graphite was mixed with H_2SO_4 (240 mL) and H_3PO_4 (27 mL) and stirred for 30 min. After that, 12 g $KMnO_4$ was slowly added to the above mixture in an ice bath and reaction was carried out at 35 °C under stirring for 1 h. Subsequently, 160 mL DI water was slowly added to complete the middle temperature oxidation process. For high-temperature oxidation reaction at 95 °C, 12 mL of 30 wt% H_2O_2 was added until the solution turned bright yellow after 30 min. Finally, the resultant solution was cooled to room temperature, and subsequently washed three times with 400 mL of 10 wt% HCl, followed by dialysis in a dialysis bag for 7 days to clear away impurities for further use.

2. Synthesis of $Ti_3C_2T_x$ MXene nanosheets

The two-dimensional $Ti_3C_2T_x$ MXene nanosheets were fabricated by selectively etching Ti_3AlC_2 MAX powders following the previously reported method. In a typical process, 1 g Ti_3AlC_2 powder was slowly added to a mixing solution of 1.6 g LiF powders in 20 mL of 9 M HCl solution, and the reaction was maintained at 35 °C for 24

h under magnetic stirring (350 rpm). Subsequently, the products were washed three times with HCl solution followed by washing with DI water several times and centrifugation at 5000 rpm until the pH of the supernatant reached nearly 7. Furthermore, the produced clay-like deposit was redispersed in DI water and further sonicated for 30 min in an ultrasonic cell pulverizer with 70% power (Ningbo Xinzhi, China, JY88-IIN, 500 W) to obtain a stable $Ti_3C_2T_x$ MXene colloidal solution with a dark green color. Finally, the mixture was vacuum-filtrated and adjusted to a concentration of 10 mg/mL suspension containing only delaminated $Ti_3C_2T_x$ MXene nanosheets.

3. Wet-spinning of flexible MG fibers

During the spinning process for $Ti_3C_2T_x$ MXene/GO (noted as MG) fibers, the MG colloidal suspensions containing 16 mL of 2.5 mg mL^{-1} $Ti_3C_2T_x$ MXene and 2 mL of 5 mg mL^{-1} GO aqueous solution (20 wt% GO) was condensed to 13 mg/mL. Later, the concentrated MXene/GO suspension was loaded into a plastic syringe with a spinning nozzle (26 G, PEK tube with diameter of 0.25 mm) and injected into the coagulation bath (50 μL/min) by the syringe pump, where the coagulation bath was placed on the rotating platform at a constant speed (50 rpm) to collect the MG fiber. The coagulation bath was a mixture of 150 mL DI water and 50 mL ethanol with 5 wt% $CaCl_2$. After that, MG fiber was rinsed with DI water to remove the extra impurities, rolled onto the spool, and subsequently dried at 60 °C under vacuum for 12 h. Finally, flexible MG fiber SERS substrate was obtained. For convenience, MG fiber including 20 wt% GO was defined as MG-20. Moreover, for comparison, MG fibers with 5, 10, 30, 40 and 50

wt% GO were also fabricated using the same methods, and denoted as MG-5, MG-10, MG-30, MG-40 and MG-50, respectively.

4. Growth mechanism and optimization parameters of AuNCs on $Ti_3C_2T_x$ MXene nanosheets and MG fiber

Generally, the SERS sensitivity and uniformity of the noble metal nanoparticles not only depends on their sizes, shapes and environment but also on the distances between the nearby nanoparticles. Owing to their good reducibility, MXene nanosheets are regarded as superb substrates to produce various Au nanostructures. In this work, to elucidate the morphology and distribution of Au, $HAuCl_4$ growth solution was added to a 0.1 mg/mL $Ti_3C_2T_x$ MXene aqueous suspension for the growth of Au nanoparticles (see details from the **Experimental Section**). **Figure S16a** shows the transmission electron microscopy (TEM) image of the as-produced $Ti_3C_2T_x$ MXene@AuNCs hybrid material. It is clear that new AuNCs with an average size of 85.7 nm with complex shape corners are formed and tightly attached to the $Ti_3C_2T_x$ surfaces, in which the shape corners (high electromagnetic field) and short distances ("hot spots") between AuNCs can facilitate the enhancement and spatial homogeneity of the SERS signal. Moreover, the formed $Ti_3C_2T_x$@AuNCs hybrids were further analyzed by energy dispersive spectroscopy (EDS) mapping (**Figure S16a**). The elemental map demonstrates an obvious Au element signal that does not appear in other places, indicating the successful deposition of AuNCs on the $Ti_3C_2T_x$ MXene nanosheets. **Figure S16b** shows the high-resolution TEM (HRTEM) image of $Ti_3C_2T_x$ MXene@AuNCs hybrids, and lattice spacing are 0.269 and 0.273 nm corresponding to

(111) and (0110) for Au and $Ti_3C_2T_x$ MXenes, respectively.

To explore the growth mechanism of AuNCs formed from $HAuCl_4$ solution (0.1, 0.5, 1, 5 to 10 mM), UV-Vis absorption spectra of pure $Ti_3C_2T_x$ MXene and $Ti_3C_2T_x$ MXene/AuNCs colloidal suspensions were taken as shown in **Figure S16c**. In the 0.1 mM $HAuCl_4$ solution, the mixed colloidal suspension exhibits two absorbance peaks (**Figure S16d**). The absorbance band at 743 nm is consistent with the original characteristic peak of pure $Ti_3C_2T_x$ MXene. The other peak at 554 nm implies the formation of Au nanoparticles. With the increase in $HAuCl_4$ concentration from 0.1 to 5 mM, the color of the mixed colloidal suspension changed gradually from dark green to purple black, red pink, orange red and brownish yellow (**Figure S17**). This is confirmed by the red-shift of the LSPR peak from 554 to 562 nm, demonstrating the size increase and probably anisotropic growth of AuNCs with corners and complex structures on the surface of $Ti_3C_2T_x$ MXene nanosheets (**Figure S16a** and **Figure S18**). Nevertheless, the color of the suspension gradually becomes clear when the concentration of $HAuCl_4$ further reaches 10 mM, indicating the complete consumption of functional groups on the $Ti_3C_2T_x$ MXene during the reduction of AuNCs.

Figure S19a-e show the SEM images of MG/AuNCs fibers formed in different growth solutions (0.1, 0.5, 1, 5 and 10 mM) of $HAuCl_4$. As demonstrated in **Figure S19a**, small sized AuNCs initially appear on the MG fiber surface immersed in 0.1 mM $HAuCl_4$ growth solutions for 2 min, demonstrating the chemical origin of $Ti_3C_2T_x$ MXene were not altered during the fabrication process of MG fibers with wet spinning and condensing steps. As the concentration of $HAuCl_4$ is increased to 1 mM, the

average size of AuNCs gradually increased from ~97 nm to ~138 nm (**Figure S19a-c** and **Figure S20a-c**), and the corresponding coverage of AuNCs increased substantially from 16.3% to 76.7% (**Figure S21**). According to the previous research, higher coverage of noble metal nanoparticles implies denser hot spots and stronger plasma coupling. Accordingly, the SERS R6G molecules (10^{-4} M) on the MG/AuNCs fibers are significantly approved with the increase of concentration of $HAuCl_4$ solution (**Figure S22** and **Table S1**). Particularly, for MG/AuNCs-1 fiber, due to the synergistic EM enhancement within the "hot spots" between the nearby AuNCs and their corners, the Raman intensity and EF_{exp} of R6G molecules reached 1.5×10^4 a.u. and 2.01×10^9 respectively (**Table S1** and **Figure S22**). However, with the further increase in the concentration of $HAuCl_4$ solution from 1 mM to 10 mM, the closed AuNCs on the fiber starts to merge due to the size increase of AuNCs (**Figure S19d-e**, **Figure S20 d-e** and **Figure S21**). It leads to the loss of plasmonic hot spots across the fiber surface, as evidenced by the decreased EF_{exp} of R6G on the MG/AuNCs-5 (5.44×10^8) and MG/AuNCs-10 (2.12×10^8) fiber (**Figure S22b** and **Table S1**). Moreover, to reveal the depth distribution of formed AuNCs in fiber substrate, the crossed sectional morphology and elemental mapping of MG/AuNCs-1 fiber were characterized by SEM and EDS. As shown in Figure **S23a** and **b**, the AuNCs are prominently distributed on the surface rather than the interior of MG fiber since there are no spaces to allow the growth of AuNCs in the closed packed structure of the MG fiber core, which resulted in the facile charge transfer from the substrate to the analytes to enhance the SERS signal.

5. Detection of R6G deposited on MG/AuNCs SERS substrate

SERS and Raman spectra of the samples were obtained using an Alpha300R confocal Raman microscope (WI Tec) with an excitation wavelength of 532 nm. In all tests, unless specifically noted, the laser power was 0.1 mW, the specification of the objective was ×50 L, and the acquisition time was kept at 5 s for all samples. A series of R6G ethanol solutions with concentrations from 10^{-4} M to 10^{-11} M were employed as the probe molecules. For a typical SERS sample preparation, the produced MG/AuNCs series fibers were cut into 3 cm in length, and 10 μL R6G ethanol solution was then dropped on its surface. Subsequently, the sample was left undisturbed for 10 min and washed with ethanol to remove the nonspecific adsorption of R6G molecules. The SERS spectra were measured at 5 random spots of each sample. For comparison, a 10^{-4} M R6G ethanol solution was dropped on the surface of the MG-20 fiber, and all other procedures were the same as those used for MG/AuNCs fiber measurement. Moreover, to evaluate the EF from experiment (denoted as EF_{exp}), 10^{-3} M R6G solution was drop cast onto the glassware, and dried at room temperature for 12 h before the Raman test.

6. Detection of nitroexplosives deposited on MG/AuNCs SERS substrate

To detect the nitroaromatic-type explosives, the produced MG/AuNCs-1 fiber was first immersed in 10^{-6} M L-cysteine aqueous solution for 12 h and dried at 60 °C for 24 h to graft the thiol group in L-cysteine molecules on the surface of AuNCs in MG/AuNCs fiber. To analyze the TNT molecules, 10 μL TNT acetonitrile solutions

with different concentrations (0.1, 0.5, 1, 5, and 10 μM) were separately dropped on the surface of L-cysteine modified MG/AuNCs-1 (noted as MG/AuNCs-1-C) respectively, and subsequently left undisturbed for 10 min and finally washed with acetonitrile solution to remove the nonspecific adsorption of TNT molecules. For comparison, unmodified MG/AuNCs-1 was also used as SERS substrate for detecting of TNT molecules. Moreover, to investigate the selectivity of fiber substrates, four other types of Tetryl, DNT, NB and 4-NTP interfering molecules were also employed. All the other procedures for SERS detection were the same as those for R6G molecules.

To verify the actual SERS application of sample, 100 μL of TNT acetonitrile solution with different concentrations (0.1~100 μM) were dropped onto the finger and dried at room temperature respectively. Then the acetonitrile solvent (~100 μL) was added to the surface of the fingerprint or sample bag to redissolve the explosive and collected with slowly and carefully wiped. Finally, a 3 cm MG/AuNCs-1-C fiber was taken and pinched by hand to form a loop at both ends for sampling. In Raman tests, the fibers were fixed on glassware for further SERS analysis. Moreover, sample bags contaminated with tetryl molecules was also used for the SERS analysis, where the experimental procedure was the same as described above.

7. Theoretical Calculation

Commercial software (COMSOL) combined with finite element method (FEM) was used to simulate the theoretical electromagnetic field intensity. The geometric simulation models were set based on the practical morphology of the MG/AuNCs-1 fiber substrate, where octagonal AuNCs were employed to model the shapes of AuNCs

acquired by TEM, and the corresponding height of each corner in AuNCs was measured as 18 nm. The AuNCs diameter (120 nm) and interparticle distance (2~20 nm) were deduced from the SEM results. The incident wavelength was defined as 532 nm, and the gold parameter values were provided by the software. All outside boundaries were regarded as perfectly matched boundary layers (PMLs) to achieve absorbing boundary conditions, and all AuNCs were divided into free tetrahedral grids to maintain their shape.

8. Calculation of the enhancement factor

The following equation was used to calculate the EF_{exp}:

$$\text{EF}_{\text{exp}} = \frac{(I_{SERS}/N_{SERS})}{(I_{REF}/N_{REF})} \tag{S1}$$

Where N_{SERS} and N_{REF} are the number of probe molecules in the excitation volume of the MG/AuNCs fiber substrate and reference, respectively. I_{SERS} and I_{REF} are respectively the Raman signal intensities at 612 cm^{-1} obtained from 10^{-4} M R6G molecules on the MG/AuNCs fiber substrate and 10^{-3} M R6G molecules on bare glassware, while sample was excited under 532 nm laser irradiation. For the calculation of N_{SERS}, 0.1 μl (V_1) from 10^{-4} M (C_1) R6G solution was adsorbed on the surface of the 16 mm^2 fibers (S_1). The Raman's laser spot diameter was about 5 μm (d). The number of excited probe molecules were calculated in the following way:

$$N_{SERS} = (\frac{\pi d^2}{4 \times S_1}) \times V_1 \times C_1 \times N_A \tag{S2}$$

For the calculation of N_{REF}, the laser was passed through the R6G solution ($C_2=10^{-3}$ M), and the illuminated volume (V_2) was about 6.25×10^{-14} m^3. The number of probe molecules being illuminated in the reference Raman measurement was calculated as:

$$N_{REF} = V_2 \times C_2 \times N_A \qquad \text{(S3)}$$

From this, the EF_{exp} of different samples can be calculated separately.

9. Tables

Table S1. EF of R6G molecules (10^{-4} M) on MG/AuNCs fiber substrates produced by different concentrations of $HAuCl_4$ growth solutions.

Concentration of $HAuCl_4$ (mM)	SERS Intensities (a.u)	EF
10	6.5×10^3	2.41×10^8
5	9.3×10^3	3.35×10^8
1	1.5×10^4	2.01×10^9
0.5	5.5×10^3	5.44×10^8
0.1	1.3×10^3	2.12×10^8

Table S2. XPS peak fitting results from pure MG and MG/AuNCs-1 fibers.

	MG fiber			MG/AuNCs-1 fiber	
Region	Binding energy (eV)	Assigned to	Region	Binding energy (eV)	Assigned to
Ti $2p_{3/2}$	454.06	C-Ti-OH	Ti $2p_{3/2}$	454.07	C-Ti-OH
$(2p_{1/2})$	(460.27)		$(2p_{1/2})$	(460.17)	
	455.08	Ti-C		455.15	Ti-C
	(461.19)			(461.10)	
	455.99	C-Ti-O		456.12	C-Ti-O
	(462.08)			/	
	457.25	Ti-O		458.13	Ti-O
	/			(463.12)	
O 1s	529.65	-OH	O 1s	529.97	-OH
	531.16	Ti-O		530.81	Ti-O
	532.40	Ti-C-O		531.96	Ti-C-O
F 1s	684.08	Ti-F	/	/	/
Au $4f_{7/2}$	/	/	Au $4f_{7/2}$	83.17	AuNCs
$(4f_{5/2})$	/	/	$(4f_{5/2})$	(86.82)	

10. Figures
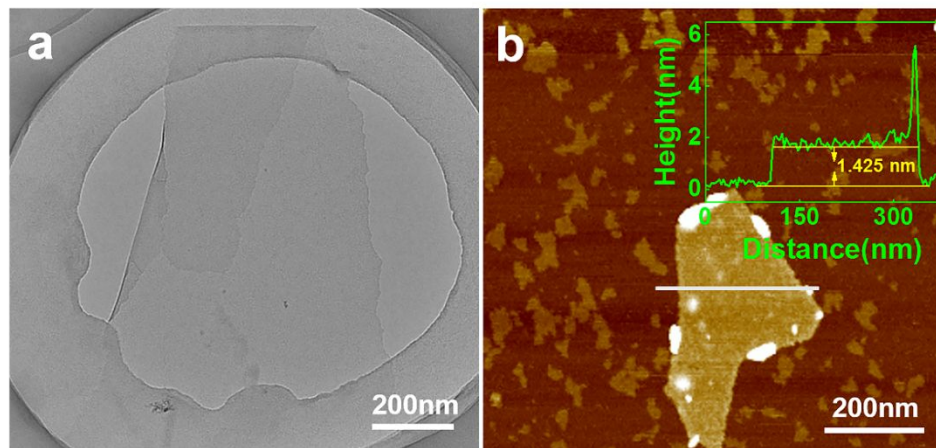
Figure S1. (a) TEM and (b) AFM images of produced $T_3C_2T_x$ MXene nanosheets. Inset in (b):

height profiles across $Ti_3C_2T_x$ MXene nanosheets by white-dashed line.
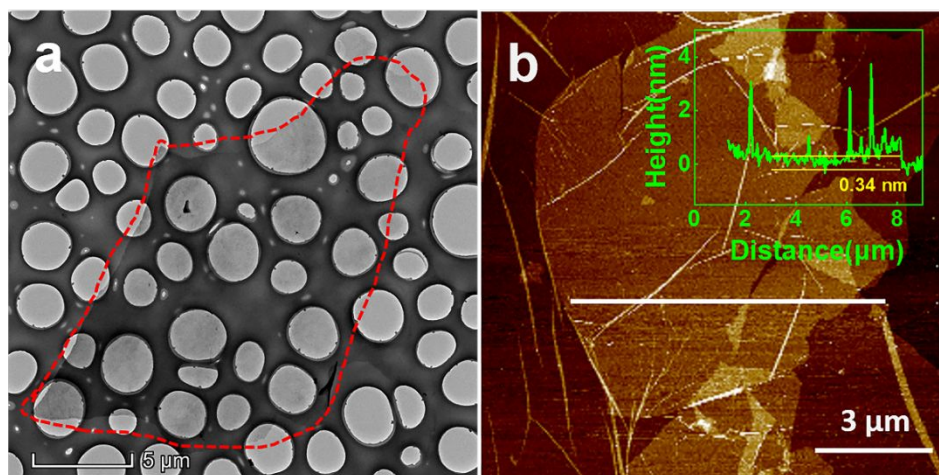
Figure S2. (a) TEM and (b) AFM images of GO nanosheets. Inset in (b): height profiles across the

GO nanosheets by white-dashed line.
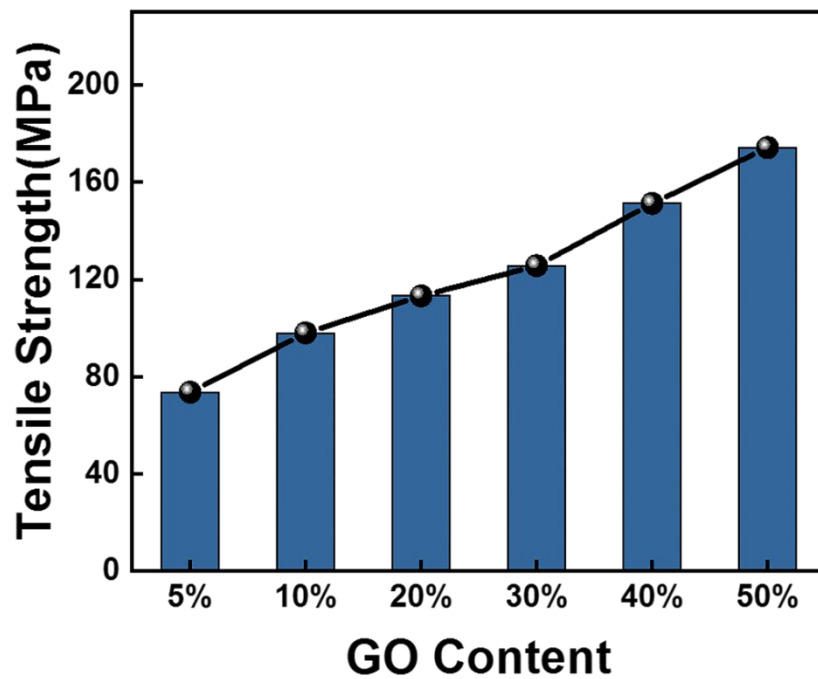
Figure S3. Tension strength of flexible MG fibers as functions of the content of graphene oxide

(GO) within the MG fibers.
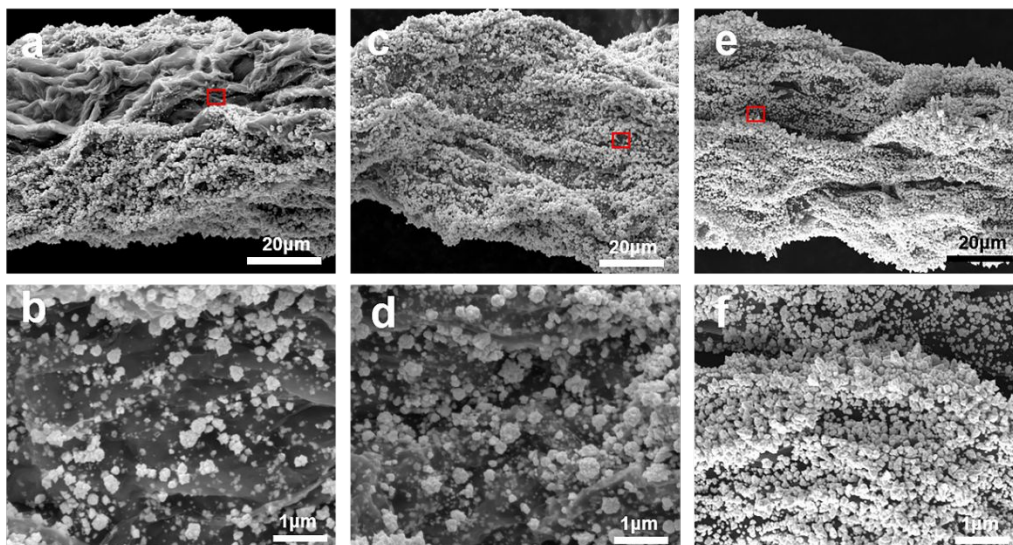
Figure S4. SEM images of MG/AuNCs fibers fabricated by MG fibers including different content of GO, such as (a) 40 wt%, (c) 30wt% and (e) 10 wt%. (b), (d) and (f) their corresponding SEM images of enlarged area outlined by the red rectangle.
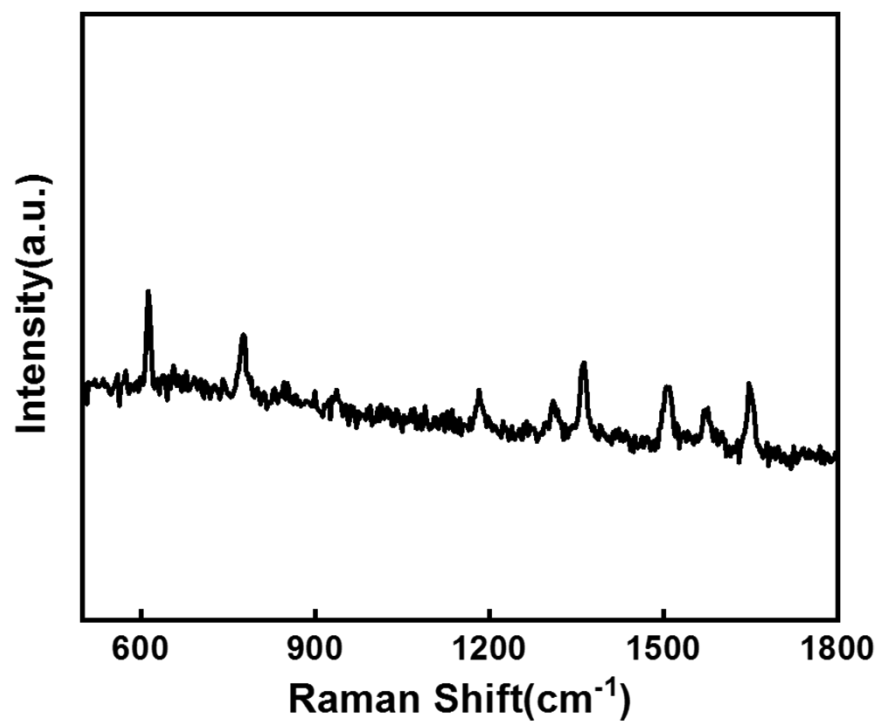
Figure S5. SERS spectrum of R6G molecules (10^{-11} M) on the MG/AuNCs-1 fiber substrate.
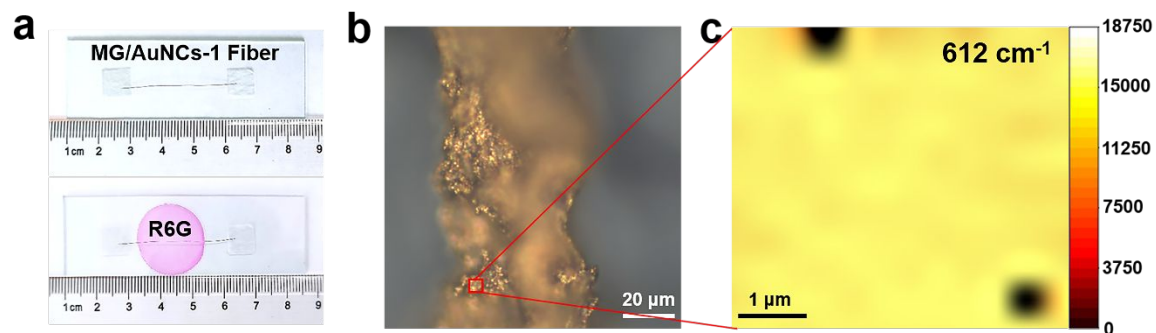
Figure S6. (a) Photographs of the measurement setup for the SERS test of R6G molecules on the fiber. (b) Optical image of the MG/AuNCs-1 fiber and the corresponding Raman mapping were carried out within the 5 x 5 μm² area marked by red square. (c) SERS mapping based on the intensity of the 612 cm⁻¹ characteristic peak of R6G molecules.
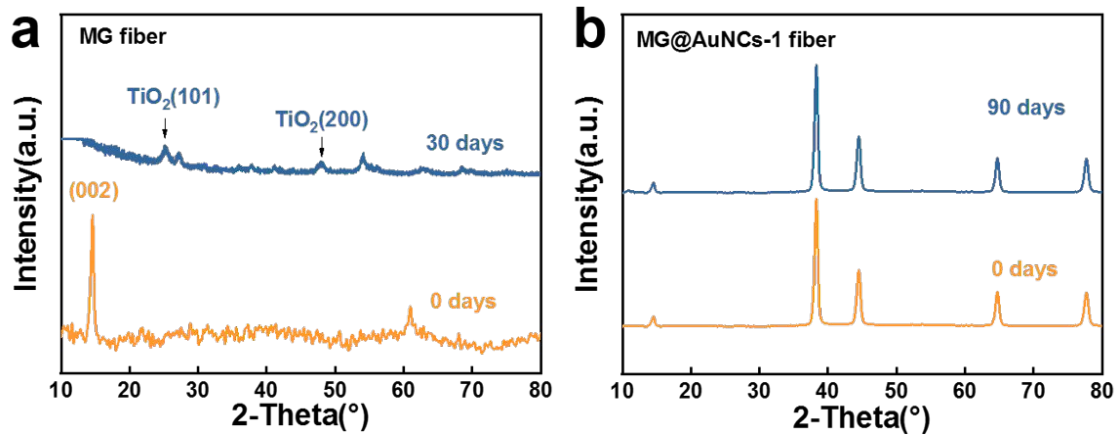
Figure S7. XRD patterns of MG fiber substrate (a) exposed to air for 0 and 30 days, and

MG/AuNCs-1 fiber substrate (b) exposed to air for 0 and 90 days, respectively.
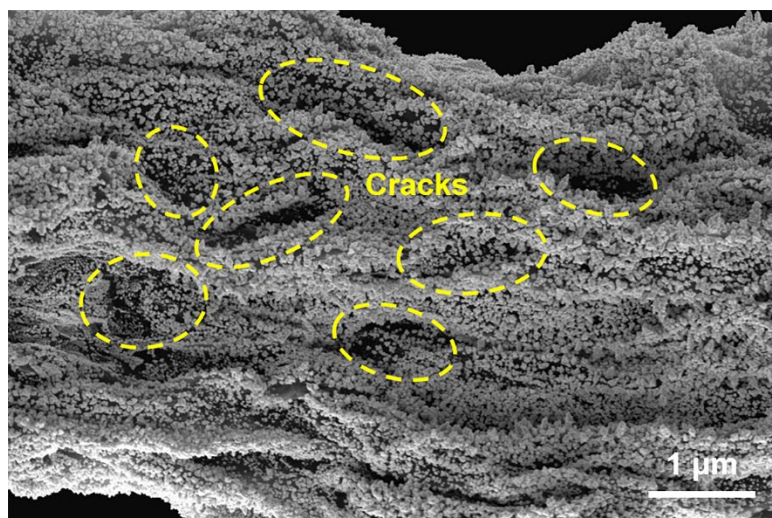
Figure S8. SEM image of MG/AuNCs-1 fiber substrate after 500 bending cycles.
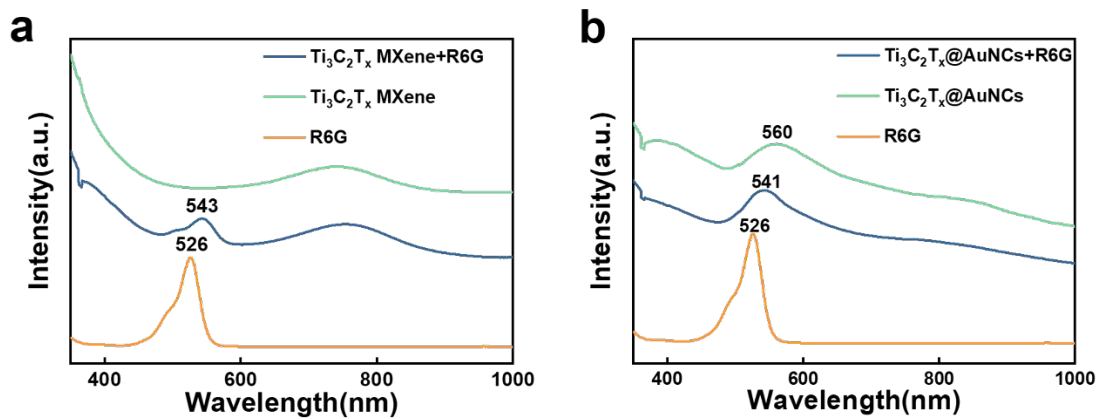
Figure S9. Comparison of UV-vis spectra of (a) mixture of $Ti_3C_2T_x$ MXene and R6G molecules, pure $Ti_3C_2T_x$ MXene and pure R6G solution; (b) mixture of $Ti_3C_2T_x$@AuNCs and R6G molecules, pure $Ti_3C_2T_x$@AuNCs and pure R6G solution.
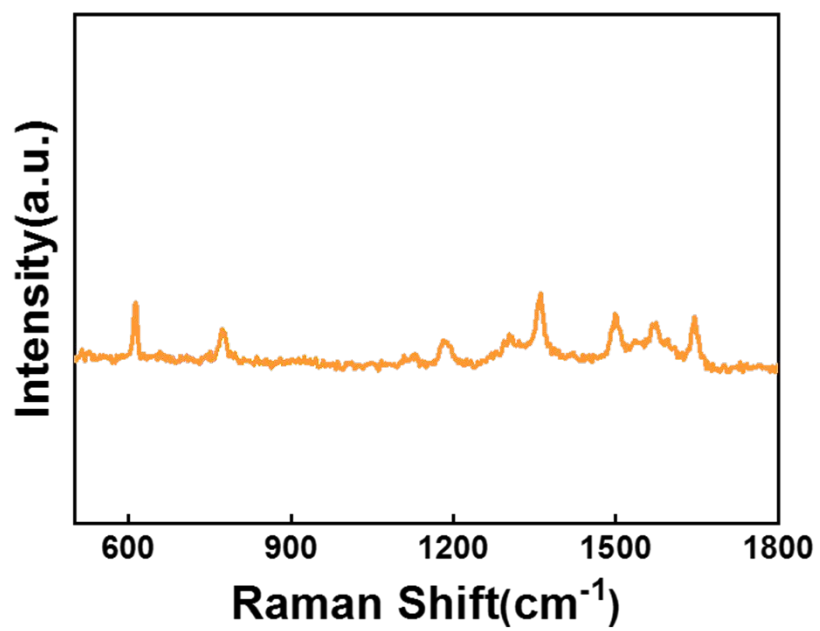
Figure S10. SERS spectra of R6G (10^{-4} M) on the pure MG fiber.
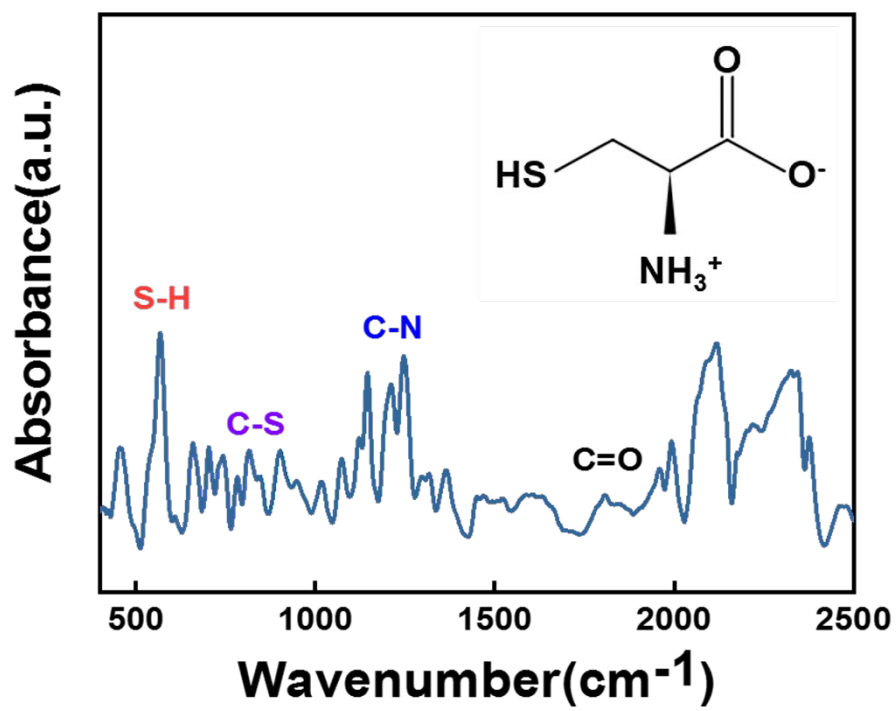
Figure S11. The infrared spectrum of L-cysteine-modified MG/AuNCs-1 fiber.
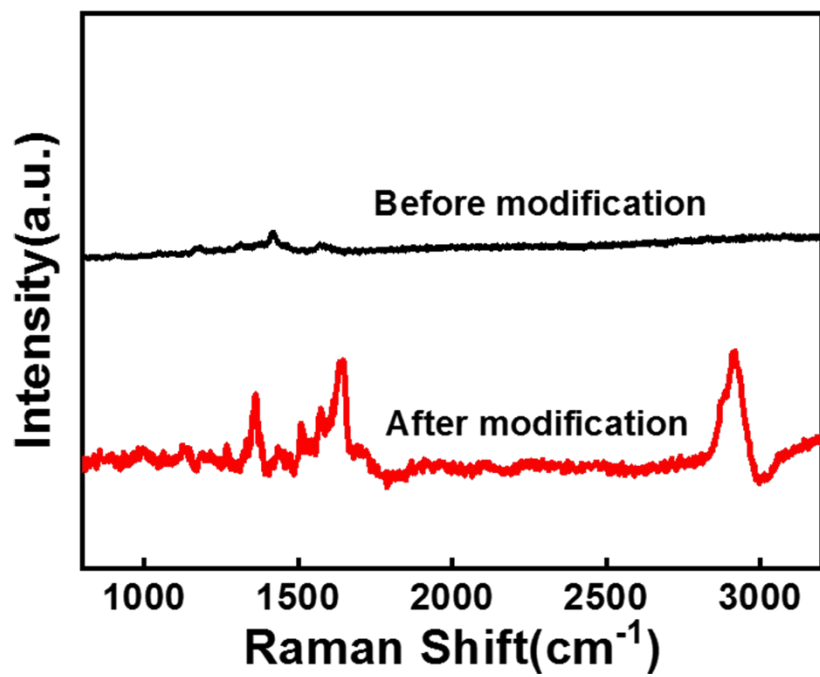
Figure S12. SERS spectra of TNT (10 μM) on MG/AuNCs-1 fiber before and after modification of

L-cysteine molecules.
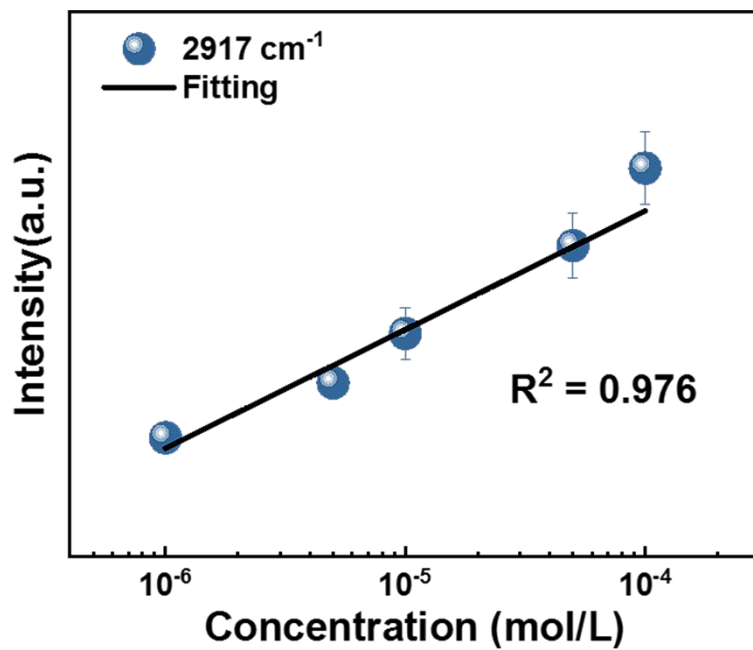
Figure S13. The relationship between SERS intensity and concentration described by the 2917 cm^{-1}

peak of TNT on flexible MG/AuNCs-1-C fiber substrate.
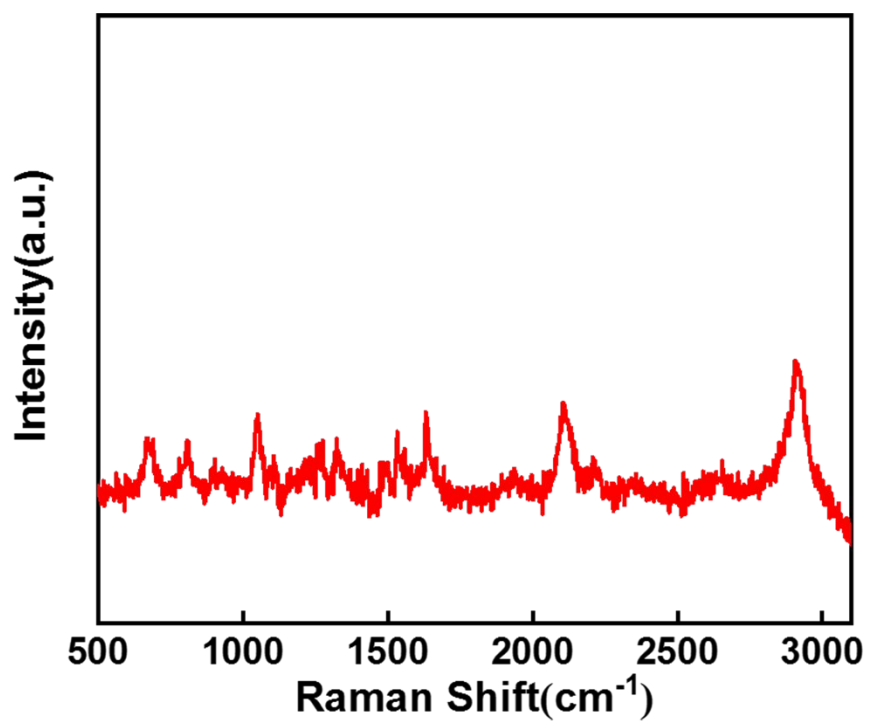
Figure S14. SERS spectrum of TNT (0.1 μM) on the surface of flexible MG/AuNCs-1-C fiber
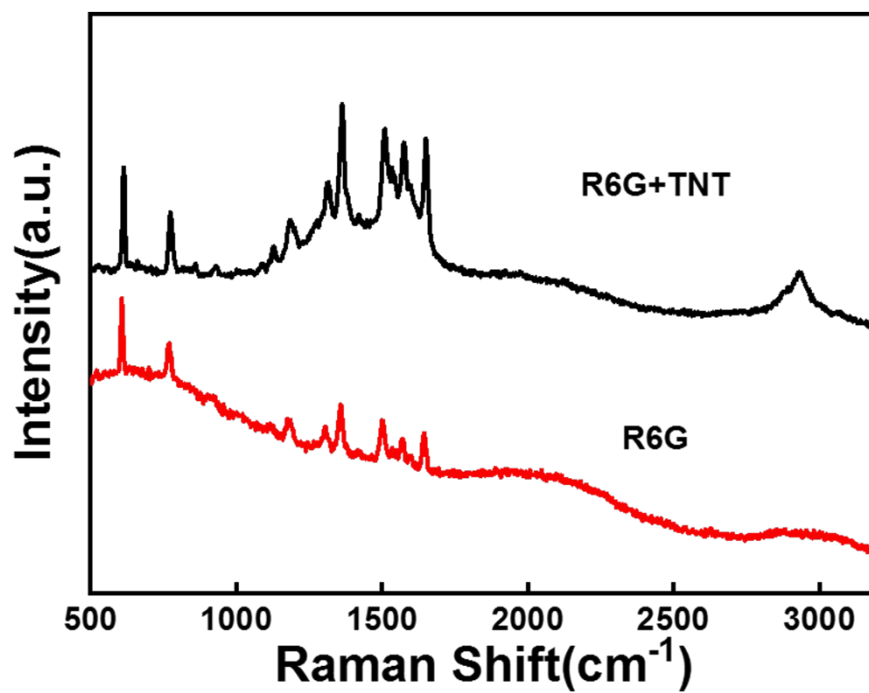
substrate.

Figure S15. SERS spectra of R6G, and mixture of R6G and TNT molecules on the surface of

MG/AuNCs-1-C fiber substrate respectively.
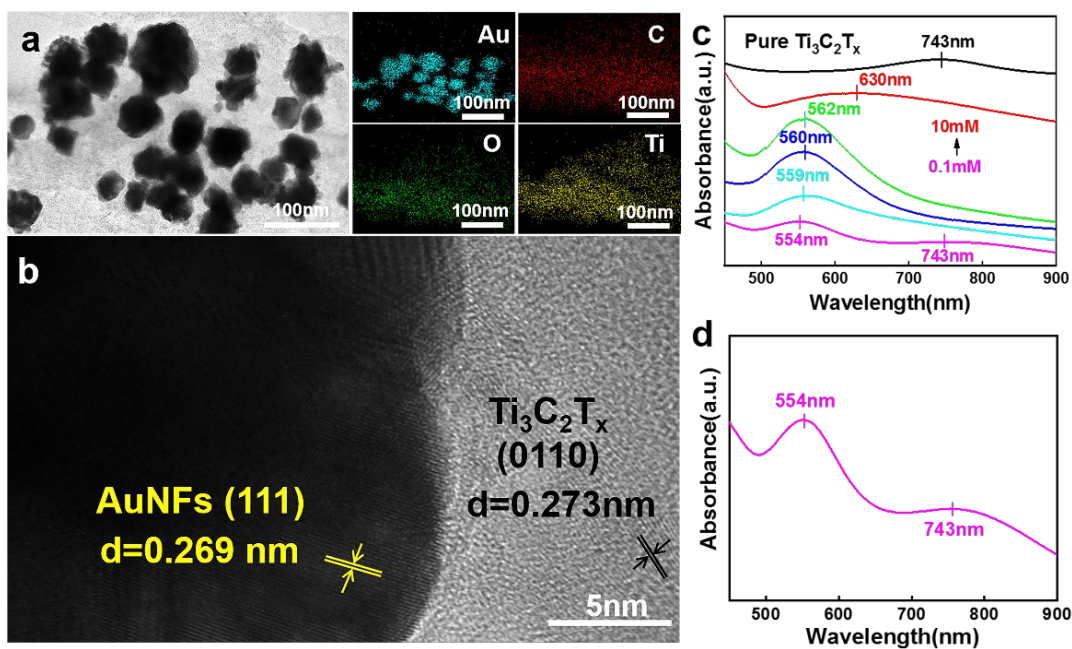
Figure S16. (a) TEM image of $Ti_3C_2T_x$ MXene@AuNCs hybrid nanosheets and the corresponding EDS mapping of Au, C, O and Ti elements. (b) High-resolution TEM image of $Ti_3C_2T_x$ MXene@AuNCs hybrid. (c) UV-Vis-NIR absorption spectra of $Ti_3C_2T_x$ MXene colloidal suspensions after adding different concentrations of $HAuCl_4$ solutions in the range from 0, 0.1, 0.5, 1, 5 to 10 mM. (d) UV-Vis absorption spectra of $Ti_3C_2T_x$ MXene colloidal suspension within 0.1 mM $HAuCl_4$ growth solution.

Figure S17. The digital image of Ti$_3$C$_2$T$_x$ MXene colloidal suspensions after adding different concentrations of HAuCl$_4$ solutions in the range of 0 mM to 10 mM.
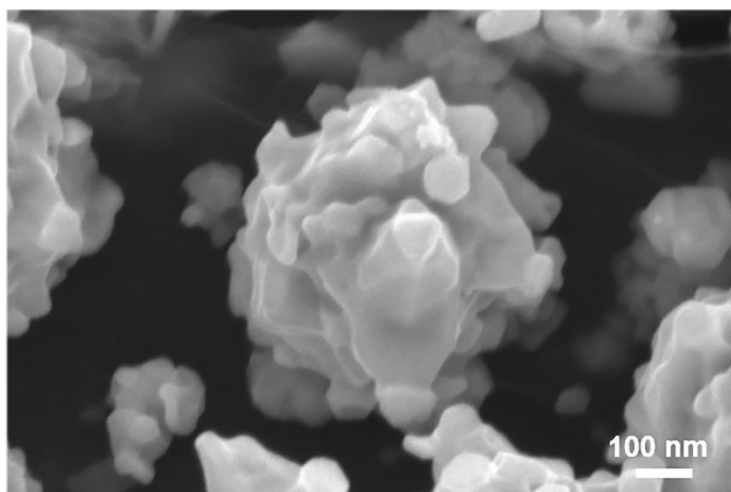
**Figure S18**. The SEM image of single AuNC on the surface of MG fiber.
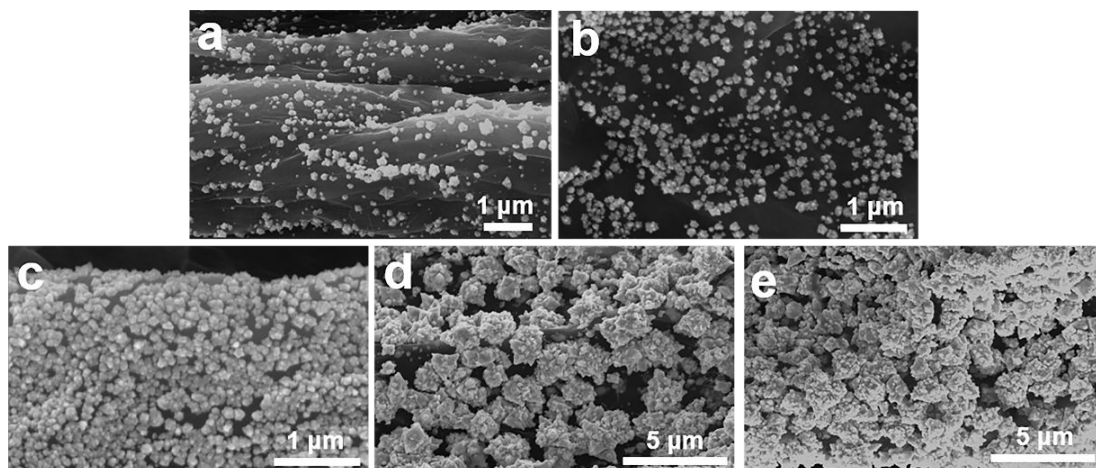
Figure S19. SEM images of MG/AuNCs fiber substrates produced by different concentrations of HAuCl$_4$ growth solutions, such as 0.1 mM for (a), 0.5 mM for (b), 1mM for (c), 5 mM for (d) and 10 mM for (e).
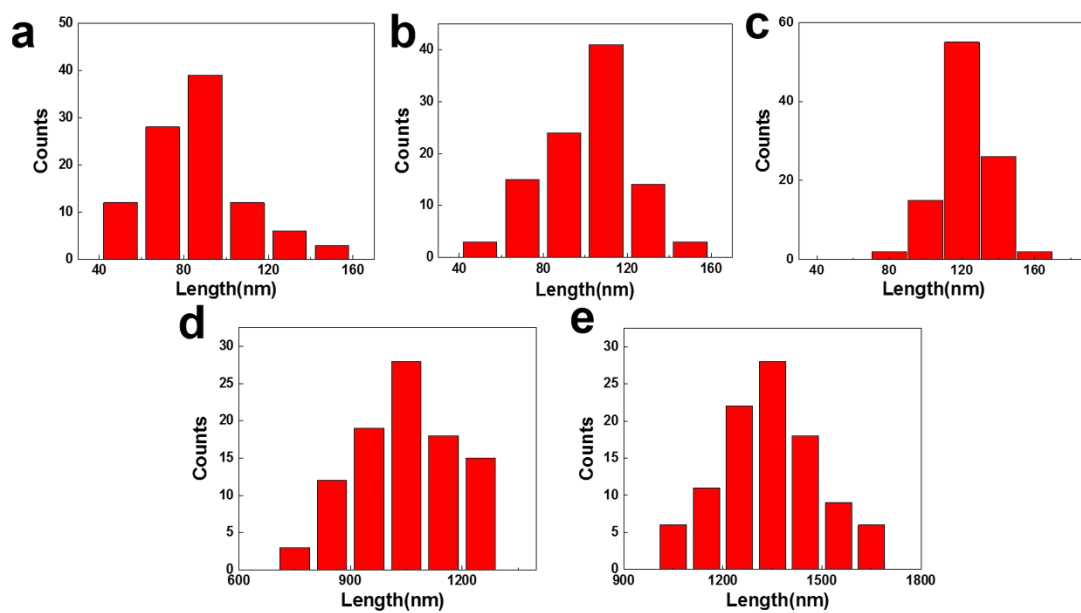
Figure S20. Size distribution of AuNCs on the surface of MG fibers at different concentrations of HAuCl$_4$ solutions: (a) 0.1 mM, (b) 0.5 mM, (c) 1 mM, (d) 5 mM and (e) 10 mM. 100 counts were performed for each statistical analysis.
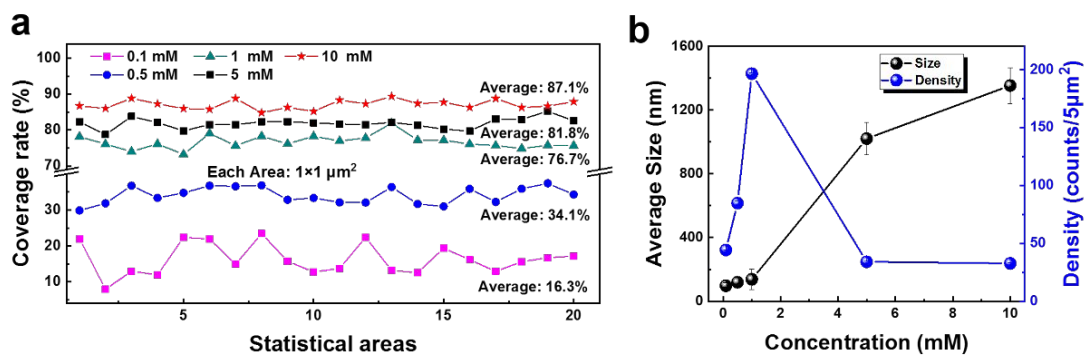
Figure S21. (a) Coverage of AuNCs on MG fiber surface at different concentrations of HAuCl$_4$ solutions. Each statistical analysis was performed in 20 random 1×1 μm^2 zones. (b) Relationship between the size of AuNCs and their corresponding density as functions of different concentrations of HAuCl$_4$ solutions, respectively.
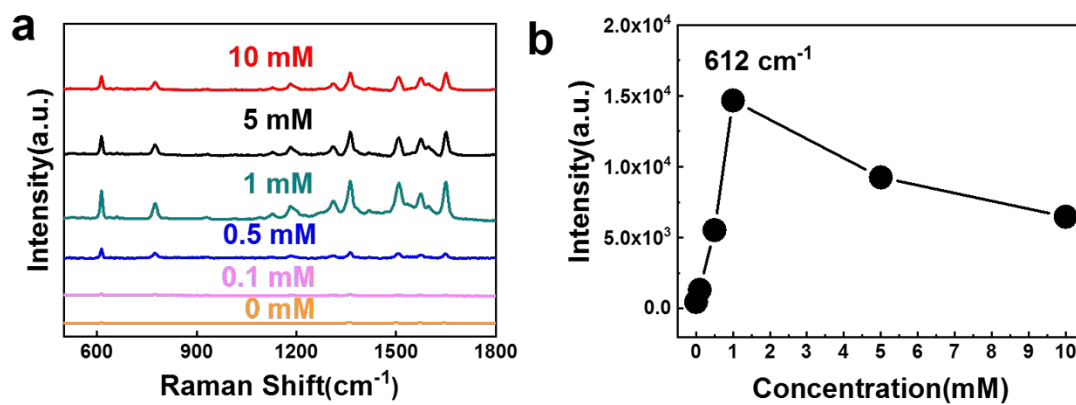
Figure S22. (a) SERS spectra of R6G (10^{-4} M) on the MG/AuNCs fibers synthesized in different concentrations of $HAuCl_4$ growth solutions. (b) The corresponding Raman intensities at peak of 612 cm^{-1} as a function of different concentrations of $HAuCl_4$ growth solutions.
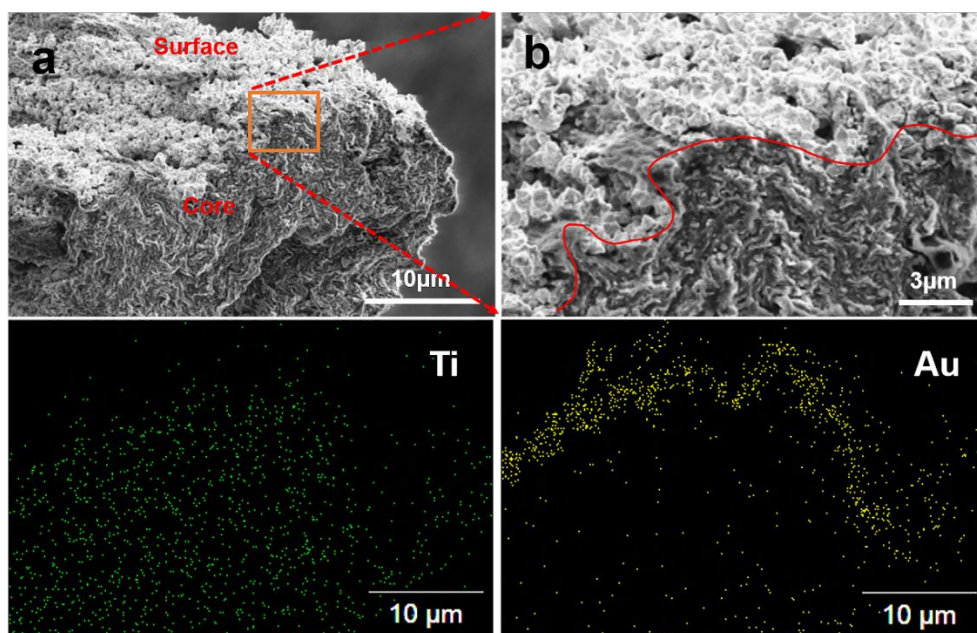
Figure S23. (a) Cross-sectional SEM image of MG/AuNCs-1 fiber and their corresponding EDS mapping of Ti and Au elements. (b) The enlarged view of cross section of MG/AuNCs-1 fiber circled by the rectangle shape with orange color, where a redline curve in (b) was used to guide the interface between AuNCs and core area of fiber.